

APPLICATION OF ABLATION COOLING TO CATARACT SURGERY TECHNIQUE USING ALL-FIBRE BURST-MODE LASER

A THESIS SUBMITTED TO
THE GRADUATE SCHOOL OF ENGINEERING AND SCIENCE
OF BILKENT UNIVERSITY
IN PARTIAL FULFILLMENT OF THE REQUIREMENTS FOR
THE DEGREE OF
MASTER OF SCIENCE
IN
ELECTRICAL AND ELECTRONICS ENGINEERING

By
Denizhan Koray Kesim
January, 2016

APPLICATION OF ABLATION COOLING TO CATARACT
SURGERY TECHNIQUE USING ALL-FIBRE BURST-MODE
LASER

By Denizhan Koray Kesim

January, 2016

We certify that we have read this thesis and that in our opinion it is fully adequate,
in scope and in quality, as a thesis for the degree of Master of Science.

F. Ömer İlday(Advisor)

Ergin Atalar

Nurullah Çağıl

Approved for the Graduate School of Engineering and Science:

Levent Onural
Director of the Graduate School

ABSTRACT

APPLICATION OF ABLATION COOLING TO CATARACT SURGERY TECHNIQUE USING ALL-FIBRE BURST-MODE LASER

Denizhan Koray Kesim

M.S. in Electrical and Electronics Engineering

Advisor: F. Ömer İlday

January, 2016

Cataract is the most common cause of preventable blindness in the world. Each year more than 19 million operations are performed to treat cataract. While history of cataract surgery goes as far as 2000 BC, beginning with the last quarter of the 20th century, cataract surgery procedures has benefited from advancements in ophthalmology such as phaco-emulsification, intra-ocular lens (IOL) and precision tools. There was another transformation of special interest to this thesis: In 2009, the cataract surgery was performed on a human being using a femtosecond laser for the first. Use of lasers has since gathered much attention for their high precision and repeatability in cataract surgery, but there are still challenges that their prevent wide-spread adaptation. The leading challenges can roughly be group into technical and fundamental. The technical challenges include the high cost, complexity and bulk of the associated laser technology. The more fundamental challenges relates to the interaction of ultrafast pulses with tissue. Namely, there is always interest in further reducing collateral damage and post-operation complications, which can potentially be done by reducing required pulse energies or average powers. Such an advance would also simplify the required laser technology indirectly. The principle aim of thesis has been to help overcome these challenges.

In this thesis, a Yb-doped fibre laser system generating femtosecond pulses was designed to exploit recently discovered ablation-cooled laser-material removal technique. The laser system was then integrated with optical coherence tomography (OCT) for in-situ imaging during cataract surgery. In order to keep required average powers low, ablation-cooled regime is accessed through burst-mode operation of the laser. This custom-built system aims to enhance further the procedure

with lower collateral tissue damage, cleaner, efficient cuts with a compact and robust structure. Preliminary experiments have been conducted on blood agar, plexiglas and extracted bovine eyes comparing the new ablation-cooled regime with the traditional regime. All experiments indicate that this regime achieves ablation with smaller pulse energies and reduced thermal effects to nearby tissue. Specifically, the pulse fluency required for corneal incision is decreased by a factor of ~ 15 compared to previous publications. The system has been developed into a transportable laboratory prototype, ready to be used by medical doctors through custom-developed computer control software.

Keywords: Fibre Laser, OCT, Burst Mode, Biomedical Application, Tissue Processing, Cataract Surgery, Ablation Cooling.

ÖZET

ABLASYON SOĞUTMANIN KATARAKT AMELİYATI İÇİN KÜME-MODLU FİBER LAZER İLE UYGULAMASI

Denizhan Koray Kesim

Elektrik Elektronik Mühendisliği, Yüksek Lisans

Tez Danışmanı: F. Ömer İlday

Ocak, 2016

Katarakt önlenabilir körlüğün en yaygın sebebidir. Her yıl 19 milyondan fazla insan katarakt ameliyatı olmaktadır. Bu operasyonun tarihi millattan önce 2000 yıllarına dek uzanmasının yanında, 20. yüzyılın son çeyreğinde başlamak üzere, katarakt ameliyatları için kullanılan yöntemler de göz bilimindeki önem teşkil eden gelişmeler sayesinde (intraoküler lens, fako emülsifikasyon, hassas cerrahi aletler) önemli aşamalar kaydedildi. Bu tezin üzerinde özel olarak durduğu bir değişim daha var: 2009 yılından bu yana femtosaniye laser teknolojisi ilk defa katarakt ameliyatlarında insanlar üzerinde uygulandı. Lazerlerin kullanımı, özellikle yüksek hassasiyetleri ve tekrarlanabilirlikleri açısından tercih ediliyor. Femtosaniye katarakt cerrahisi teknolojisinin gelişmeye açık tarafları yaygın kullanılabilmesinin önüne geçiyor. Bu zorluklar temel ve teknik olarak ikiye ayrılabilir. Teknik zorluklar olarak, yüksek maliyet, sistemin boyuları ve karmaşıklığı gösterilebilir. Daha temel zorluklar ise ultrahızlı atımların doku ile olan etkileşiminden kaynaklanmaktadır. Şöyle ki, istenmeyen çevresel hasarların ve operasyon sonrası komplikasyonların azaltılması her zaman istenilen bir durum, ki bu da potansiyel olarak atım enerjisini ya da ortalama gücü düşürerek yapılabilir. Bu gelişmeler ayrıca gereken lazer teknolojisinin de basitleşmesine dolaylı yoldan katkı sağlayacaktır. Tezin asıl amacı bu zorlukların üstesinden gelinmesine yardım etmektir.

Bu tezde, yeni keşfedilmiş lazerle ablasyon soğutmalı material kaldırmadan yararlanabilecek Yb katkılı femtosaniye fiber lazer sistemi tasarlanmıştır. Lazer sistemi katarakt ameliyatı sırasında görüntüleme yapabilmesi için optic koherans tomografi (OCT) ile entegrasyonu gerçekleştirilmiştir. Ortalama gücü düşük tutabilmek için, ablasyon soğutmalı rejim küme-modu ile sağlanmıştır. Bu özel

hazırlanmış sistem, küçültülmüş ve güvenilir olarak doku üzerindeki istenmeyen zararları en aza indirgeyerek daha temiz ve verimli kesiler oluşturabilmektir. Ön denemeler agar, pleksiglas ve ölü dana gözü örnekleri üzerinde ablasyon soğutma rejiminin geleneksel rejim ile kıyaslamak amacıyla yapıldı. Deneylerin bütünü bu rejimin atım enerjisini küçültüp ablasyonu hedefin çevresini daha az ısıtarak yaptığına işaret etmektedir. Spesifik olarak korneaya giriş için gereken atım akışı ise önceki yayınlara göre ~ 15 kat azaltıldı. Sistem, hekimlerin özel geliştirilmiş bilgisayar kontrol programı üzerinden kullanabileceği taşınabilir bir prototip haline getirildi.

Anahtar sözcükler: Fiber Lazer, OCT, Küme Modu, Biyomedikal Uygulama, Doku İşleme, Katarakt Ameliyatı, Ablasyon Soğutma.

Acknowledgement

I would like to thank Fatih Ömer İlday for opening up the opportunity for me to do research in his group. It was an invaluable experience for me that was educational academically. His advisory thought me the how to do science and conduct research properly which are not only valuable scientifically but other aspect of life too.

I specially want to express my gratitude to Hamit Kalaycıoğlu for his endless patience with me. Thanks to his knowledge and discussions, I learned a lot. The fibre laser system developed was based on burst-mode fibre lasers first demonstrated by him.

I would like to thank Can Kerse for intruducing me to group and inspiring me to do research.

I would like to thank Nurullah Çağıl and Mehmet Aşık for their valuable counselling and guidance through out whole project.

I would like to thank my parents, Servet Kesim and Bülent Kesim, and my sister, Yaprak Öykum Kesim for their endless love and support. They made me who I am today. Their place in my life is irreplaceable and most enjoyable. I would also like to thank to Begüm Akbay for her patience and support during this tiring period. Thank you for entering my life and making it more beautiful than I can ever imagine.

Last, but not least, I thank to Özgün Yavuz, Uğur Teğın, Ahmet Turnalı, Sinem Yılmaz, Onur Tokel, Gaith Makey, Ihor Pavlov, Parviz Elahi, Önder Akçaalan for their friendship and enjoyable conversations.

This work is financially supported by TÜBİTAK Project 112T980, Project 114F256 and Heath Ministry of Turkey.

Contents

1	Introduction	1
1.1	Cataract	2
1.1.1	Cataract Surgery	2
1.2	Lasers	3
1.2.1	Fibre Lasers	4
1.3	Multi-photon Absorption and Photodisruption	6
1.3.1	Ablation-Cooled Material Removal	6
2	Cataract Surgery System	9
2.1	Laser	9
2.1.1	Oscillator	10
2.1.2	Preamplifier	11
2.1.3	Power Amplifier	12
2.1.4	Compression and Laser Output	13

2.2	Electronics	14
2.3	Optical Coherence Tomography	16
2.3.1	Integration with Laser	18
2.4	Software	19
3	Methodology	21
3.1	Preparations	21
3.2	Blood Agar Experiments	22
3.2.1	Straight Cuts	23
3.2.2	Volume Ablation	23
3.3	PMMA Experiments	24
3.4	Bovine Eye Experiments (Corneal Flap)	24
4	Results	27
4.1	Agar Experiments	27
4.2	PMMA Experiments	28
4.3	Bovine Eye Experiments (Corneal Flap)	29
5	Conclusion	32
A	Detailed Laser Schematics	40

B	XYZ Stage Details	42
B.1	Elevator (Z-stage)	43
B.2	XY Stage	43

List of Figures

1.1	Gray are is coating, green area is cladding, blue is core. In double clad fibers, there is an additional layer of cladding which is shown in red	5
1.2	(a) Pulses are separated equally. Repetition rate can go from in the order of Hz to order of MHz. (b) Pulse to pulse repetition rate is typically very high (in the order of hundreds of MHz to GHz) but burst to burst repetition rate is typically much lower	8
2.1	On far left corner, oscillator box is visible. On the other left corner is grating compressor. Right side of the table is reserved for OCT probe, XY stage and elevator for experiments.	10
2.2	all-normal dispersion Oscillator: Produces 200 mW power at 91 MHz repetition rate	10
2.3	Oscillator Output Spectrum, 12 nm FWHM spectrum, 200 mW output power, 2.75 ps FWHM pulse length	11
2.4	Coupler Spectrum after stretch fibre	12
2.5	Laser Output Spectrum, 11 nm FWHM, 2 W output power, 63 ps	13

2.6	Incoming laser hits the first grating and its spectral components are separated spatially. With the help of second grating and mirror, each spectral component experience delay linearly proportional to their wavelengths, thus compressing the pulse temporally	14
2.7	Burst Mode Operation(change for new oscillator)	15
2.8	Potentiometer can adjust the DC bias from 0V to 2.7V. BASYS2 has its clocking threshold around 1.25V.	15
2.9	Different wavelengths reflected from corresponding depths and interfere with reference beam to construct the final image. Interference beam is measured by a detector array	16
2.10	Screenshot of ThorImage OCT software. It handles the data coming from OCT engine. Imaging type, resolution, speed can be chosen. Real time camera feed can also be seen within ThorImage. It has some additional filters and processing to reduce the distortions.	17
2.11	Processing beam (red) is inserted via dichroic mirror. Imaging beam (green) travels on its usual but elongated path. A programmable shutter is placed on path of processing beam.	19
2.12	Screenshot of the software. One can choose between 3 predetermined patterns with 2 different options (wall structure & raster). It can also adjust the initial height of the elevator and the intensity of OCT probe lighting.	20
3.1	Agar is placed on petri dish filled with tap water. Occasionally, few drops of water is dripped on top to prevent drying out locally.	23
3.2	Extracted cornea is place on holder. Then it is tightened with a cap (gray). Normal saline is pumped from the tubes which prevents drying out.	25

3.3	(a) A spring pattern starting from $200\ \mu$ below surface, as walls of the flap. (b) constructs the basis of the cap of corneal flap beneath the surface	26
4.1	Lower half of agar is scanned with uniform-mode and upper half is scanned with burst-mode. There are little visible modification on uniform-mode side compared to burst-mode side, seen from OCT image while there are clearly ablation lines on burst-mode side. Pulse energy is kept at $1.7\ \mu\text{J}$ in both cases.	28
4.2	Half of agar is scanned with burst-mode (left side), $1.75\ \mu\text{J}$ pulse energy and $10\ \mu\text{m}$ separation between each line. Right side is scanned with exactly same parameters, except uniform-mode instead of burst-mode with $400\ \text{kHz}$ repetition rate.	29
4.3	Uniform repetition rate at $400\ \text{kHz}$ with pulse energies $900\ \text{mW}$, $1\ \text{W}$ and $1.2\ \text{W}$ respectively. Each of them is scanned with $10\ \text{mm/s}$	29
4.4	8 pulse per burst with pulse energies 900mW , 1W and 1.2W . Each of them scanned with $10\ \text{mm/s}$ with $50\ \text{kHz}$ burst repetition rate	30
4.5	24 pulse per burst, $833\ \text{nJ}$ pulse energy, repeated at $50\ \text{kHz}$	31
A.1	Laser Oscillator	40
A.2	Laser Amplifier	41
B.1	Perspective drawings of XYZ stages, The table is able to fix both laser and XYZ stages and will be durable against perturbations. .	42

Chapter 1

Introduction

In this thesis, a novel and recently developed technique, namely, ablation-cooled material removal by ultrafast pulse burst is investigated for the first time in laser processing of biological tissue from an ophthalmologic perspective. A fibre laser system is built to test it in the context of cataract surgery. This way, an understanding of the ablation-cooled regime, its practical implementation via burst-mode operation of the laser and its comparison with uniform-mode on biological, transparent subjects will be gained. The principles of ablation-cooled regime are described elsewhere [1] and will not be covered here.

Furthermore, its practical implementation requires burst-mode operation of the laser due to finite speed of beam scanners and in order to minimize power requirements. For this reason, the terms of burst-mode and ablation-cooled material processing are used interchangeably throughout this thesis. The reader should, however, be aware that not all burst-mode operation corresponds to ablation-cooled regime and that there is a minimum repetition rate, the value of which depends on the thermal diffusivity of the target material and that the pulse energy has to be scaled according to the repetition rate [1].

It will cover the building a compact laser, its integration to a customized optical coherence tomography (OCT) system and its conversion to a capable surgical

system with uncomplicated controls since it will be delivered to a hospital to further conduct experiments on live animals. Moreover, some preliminary experiments are done as proof of principle on biological and non-biological samples. The results of these experiments are also covered in this thesis.

1.1 Cataract

Cataract is defined as loss in transparency of the lens in the eye [2]. There are a number of causes for this condition [3] but it is mostly related with aging [2, 4] and it is a common problem [5]. Cataract is responsible for about two thirds of preventable visual impairments. It affects nearly 190 million people all over the world [6]. Cataract surgery is also the most performed operation in the world [6].

In the light of these circumstances, any possible improvement over the current techniques will benefit a significant portion of the human population. These improvements can be in the name of reliability, costs, reduction of post-operation complications, and ease of use. The main focus has been on reducing the complications of operation, cost of laser systems and reduction of required laser powers, which is likely to result in reduction of post-operation complications.

1.1.1 Cataract Surgery

The surgical procedure itself is an ancient practice. First writings regarding ophthalmologic practices were found in the Code of Hammurabi though, it is not clear how they handled cataract. However it is believed, Japanese doctors were performing an operation called couching even before 2000 BC [7]. Around 500 BC, Greeks were certainly using this method. In Dead Sea Scrolls, very first written description of couching can be found.

Medical science has come a long way since ancient times. Currently opacified lens is removed and replaced with intra-ocular lenses [8], tools that allow smaller

incision [9], the state of the art technique of chaco-emulsification [10] and finally lasers to performed capsulotomy (operation on capsule of the lens of the eye) [11].

Chaco-emulsification process will be improved by developing a novel laser without changing the operation itself within the scope of this thesis. In chaco-emulsification, a small incision is made in cornea. Then, lens capsule is either removed altogether or partially. Opacified lens is broken into pieces and sucked afterwards, which can be done with ultrasound or laser depending on preferences. Finally, intra-ocular lens is placed inside the lens capsule [10].

In this procedure, the introduction of the laser is very recent 2009 [12], where capsulotomy and lens fragmentation are performed with a commercial laser [13]. Other surgical devices can take part in corneal incision too [14, 15]. Whether to employ full capabilities of a system is up to the operator who may decide to perform only capsulotomy and do the rest by other means. Today, the advances in cataract surgery continue [16] and any improvement to current situation is usually appreciated.

It is especially important to reduce the pulse energy as it would reduce the size of residual cavitation bubbles after laser processing. Residual gas bubbles can increase the internal pressure of the eye which can lead up to complications after surgery. Additionally, it is important to keep in mind that current refractive laser assisted cataract surgery systems are quite expensive, it can cost between 300,000 and 500,000 USD. Reducing the cost of such systems would make them more available for people especially in underdeveloped and developing countries.

1.2 Lasers

Light amplification by stimulated emission of radiation (LASER) is a common process to emit spatially and temporally coherent light . It can be utilized in numerous areas including telecommunication, material processing, imaging, military applications, medicine, precise measurements [17–23].

The laser was invented in 1960 with ruby as gain medium inside a resonating cavity built with mirrors [24]. Ever since, development of lasers continue with new gain materials [25], various types of cavity [26] and other physical phenomena [27] that can be exploited in favor. In addition to those, scientists realized the advantages of using pulsed laser radiation compared to continuous wave laser [28] especially for some material processing applications which would benefit from nonlinear processes at high peak intensities and low average powers which reduce thermal side effects. Furthermore, multi-photon processing is possible with pulses (Explained in 1.2). There are several ways of generating pulsed laser radiation, among which actively modulating gain (gain switching), loss (Q switching) or output of laser constitute to relatively straight forward ones.

Mode-locking is another way of generating pulse trains from laser which involves obtaining short pulses through coupling of modes inside the resonator cavity.

Further, there is passive mode-locking method as a way of generating such radiation which enables the formation of shortest pulses. Passive mode-locking where pulses are created in cavity by exploiting physical phenomena, without interfering actively [29] requires a saturable absorber [30] to achieve mode-locking.

1.2.1 Fibre Lasers

In fibre lasers, light propagates and gets amplified inside a fibre waveguide. Doping of the gain fibre determines the central wavelength of the laser. Optical fibers consist of 3 main parts: core where laser beam propagates, cladding which confines the core and coating that protects the fibre (Fig. 1.1 (a)). In some fibers double cladding (Fig. 1.1 (b)) structure allows for high power amplification.

However, nonlinearity inside the fibers produces some new challenges. Also going to higher average powers is very difficult because of heating which can damage the fibre itself. For that reason, fibre lasers could not reach high powers for a long time. As a solution, chirped pulse amplification is proposed which elevated the

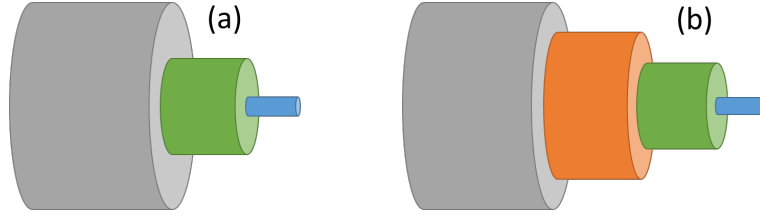


Figure 1.1: Gray are is coating, green area is cladding, blue is core. In double clad fibers, there is an additional layer of cladding which is shown in red

laser technology to next level [31]. Fibers already are highly dispersive medium, that they ease up the process. In this method laser pulses are stretched, usually exploiting this dispersive effects, before amplification. As pulses are stretched, peak powers dropped which in return allowed much greater amplifications. Additionally, mode-lock of such lasers is sensitive to environmental effects such as temperature. As a result heat stabilization and boxing is usually required.

Fibers can be bent to a certain degree which provides great advantages in terms of packaging and robustness. Fibre lasers can be more compact and stable than solid state lasers as guiding inside fibers isolates against external effects to a great extent. They can produce nearly diffraction limited beam since the wave-guide properties eliminate distortions (hence the great optical quality of the beam is achieved).

Finally, building a fibre laser is cost effective compared to solid state lasers. Considering the cost of cataract surgery systems that are currently approved, decreasing the cost of such a system would make it more available for masses. Especially for underdeveloped and developing countries, who might be reluctant to spare funds for purchasing an expensive surgery device and maintaining it.

1.3 Multi-photon Absorption and Photodisruption

In laser assisted cataract surgery, photo disruption process is resorted. In photo disruption, plasma is formed via nonlinear absorption which is followed by a shock wave, leaving a cavitation bubble behind and disrupting the tissue [32]. When a train of pulses are scanned, cavitation bubbles merge and cut through tissue. Typically, six or more photons are required for photo disruption to take place in transparent tissue. That sets up the intensity of laser beam to very high so that the probability of nonlinear absorption is substantial.

The intensity is greatest at the focal point of beam. One way to achieve this is to compress pulses as much as possible hence ultra short pulses. Shorter pulses reduce the photo disruption threshold [33]. The other way is sharp focusing the beam which would mean a more localized beam and higher intensity. This would also localize the photo disruption which limit the processed volume. A sharper focus also enables precise cutting but is very slow. In order to speed up the cutting, pulse energy is increased so that visible plasma is formed which can cleave the tissue. As a result, instead of sending pulses tangent to each other, spot separation can be increased by increasing scanning speed.

Non-linear absorption also makes subsurface modifications possible. Anywhere out of focus of beam do not go through any absorption since single photon energy is not sufficient. Propagating beam is mostly effected by scattering within the tissue.

1.3.1 Ablation-Cooled Material Removal

In literature, it is observed that higher repetition rates give better ablation performances [34]. When the repetition rate exceeds a certain value that the heat diffusion time for the material target is less then the time it takes for the next pulse to arrive, laser material interaction passes to ablation-cooled regime [35].

High repetition rate leaves no time for heat diffusion on sample, a technique used in space shuttles for a long time [36, 37]. Heat trapped in ablation region from the leading pulse is ablated by consecutive pulses. This way total heat accumulation on sample is kept at minimum and more volume is removed with same pulse energies. Heat accumulated in ablated region lowers the ablation threshold in that area by pushing electron into higher energy levels. Lower ablation threshold lets usage of pulses with less energy, which in turn reduces the collateral damage. However, the average power required for such repetition rates are extremely high that it is not practical. The laser complexity and cost of the laser makes it undesirable.

As a result, burst-mode operation is adapted. In this novel operating mode, which is the unique distribution of pulses in time where a number of them are gathered in groups which in turn repeated at much lower repetition rates [38–40] (Fig. 1.2 (b)), would overcome those impracticalities. This kind of distribution of pulses may require some additional steps in laser amplifier, like pulsed pumping [39] and shaping of pulse train before amplification [41], however, overall complexity of laser would go down with need for high average power. Burst mode operation is especially beneficial in fibre lasers where it is relatively easy to get high repetition rates from oscillator.

The heat increase of the material due to ablation is mostly related to the pulse energy. Each pulse increases the temperature of the target by a certain amount while ablating. However in burst-mode operation, when it is employed in ablation-cooled regime, the temperature increase is mostly carried away with ablated material. The net temperature increase of the target, when ablated in ablation-cooled regime, will be contributed by last few pulses inside the burst instead of all of them. That is because the heat contribution by initial pulses are already gone.

A fair comparison of burst-mode operation with traditional operation mode, namely uniform-mode (Fig. 1.2), can be done by adjusting the repetition rate to be equal to effective repetition rate of burst-mode operation while keeping the pulse energy same. The effective repetition rate of burst-mode can be found by

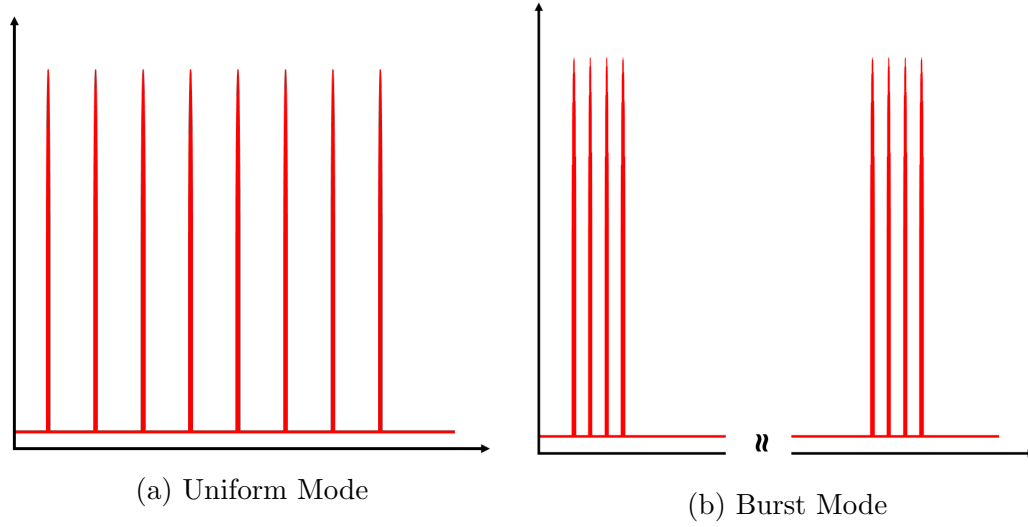


Figure 1.2: (a) Pulses are separated equally. Repetition rate can go from in the order of Hz to order of MHz. (b) Pulse to pulse repetition rate is typically very high (in the order of hundreds of MHz to GHz) but burst to burst repetition rate is typically much lower

multiplying the number of pulses inside each burst with burst-to-burst repetition rate. So both will have same average power as well as same pulse energy. This would mean the laser complexity for creating both pulse trains will be equivalent.

Properties of burst-mode mentioned above renders burst-mode operation on soft tissue most favorable. It can perform ablation on tissue with minimal thermal damage to the surrounding tissue without reducing ablated volume while increasing the speed of processing.

Chapter 2

Cataract Surgery System

2.1 Laser

A new laser system is built which can support high repetition rate bursts, enough energy to perform ophthalmic tissue processing and short pulses. Master Oscillator Power Amplifier (MOPA) architecture and Fibre medium is chosen for compactness and stability issues (Figure 2.1). Laser design consists of an all-normal dispersion oscillator,, stretch fibre, a double-clad forward pumped pre-amplifier and a double-clad backward pumped power amplifier. In addition to them, an AOM is located between pre-amplifier and power amplifier for adjusting the repetition rate.

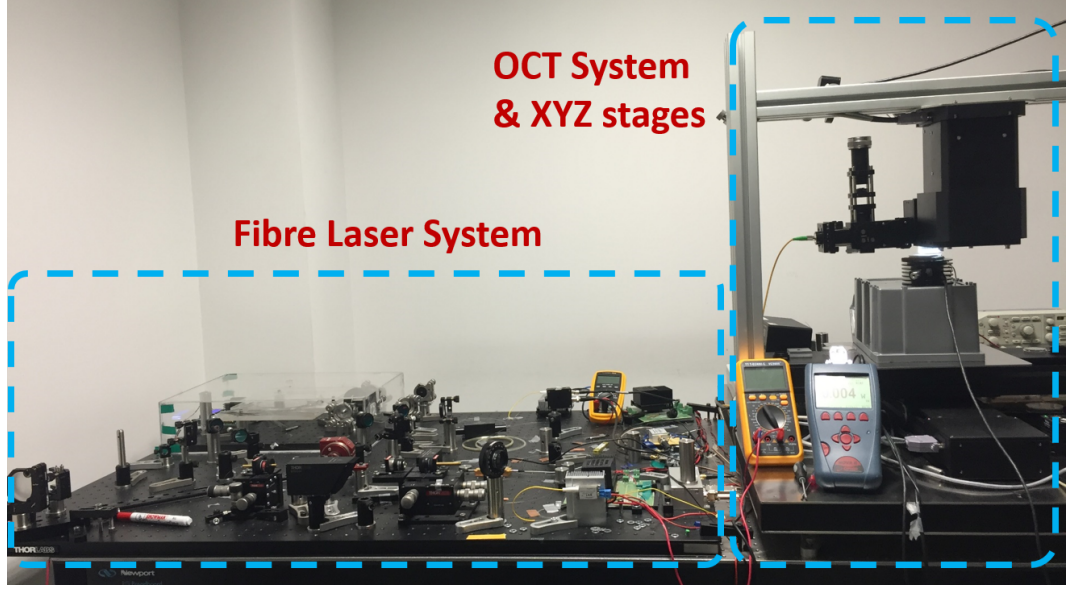


Figure 2.1: On far left corner, oscillator box is visible. On the other left corner is grating compressor. Right side of the table is reserved for OCT probe, XY stage and elevator for experiments.

2.1.1 Oscillator

Laser system is seeded by an all-normal dispersion oscillator [42] which can be seen from Figure 2.2. 30 cm 6/125 Yb-1200 fibre is used as gain medium which is pumped with single mode pump diode. 5% coupler port is connected to a detector and its signal act as clock of FPGA.

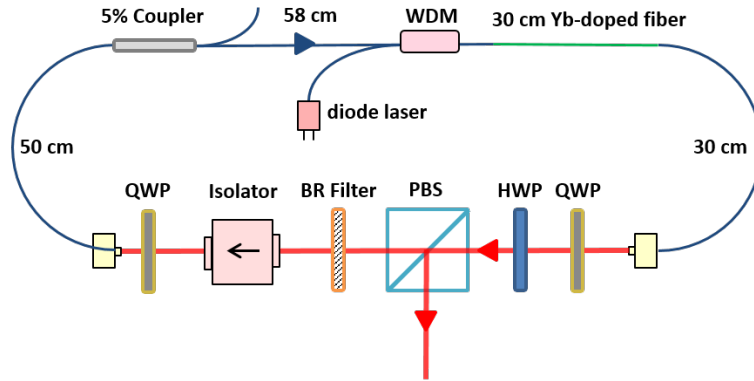


Figure 2.2: all-normal dispersion Oscillator: Produces 200 mW power at 91 MHz repetition rate

At the output, 12 nm spectral width (Figure 2.3), 185 fs transform limited pulses, 200 mW power is obtained. 140 mW of it is coupled to amplifier input fibre. The repetition rate of the oscillator is 91 MHz. A stable mode-lock can be found with self starting. It is critical to have self starting mode-locking. The laser should not be prone to possible outage and should be turned off if not needed.

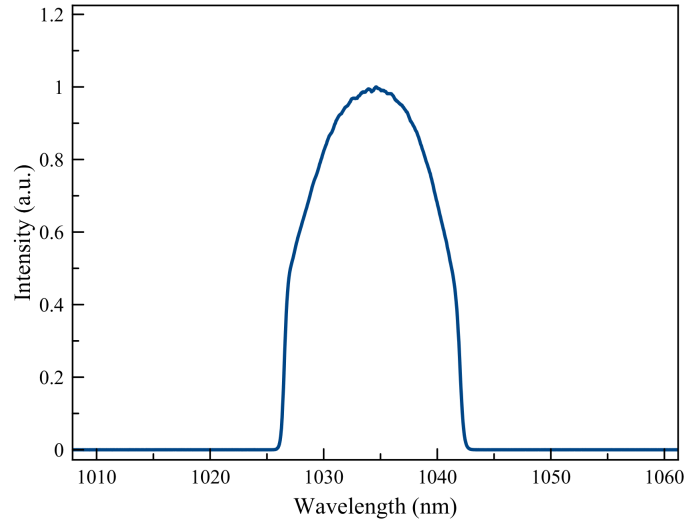


Figure 2.3: Oscillator Output Spectrum, 12 nm FWHM spectrum, 200 mW output power, 2.75 ps FWHM pulse length

Oscillator diode draws current from 5V power supply which is connected to Argenc diode driver.

2.1.2 Preamplifier

Before the acusto optic modulator (AOM) pulses need to be amplified since AOM will induce a huge loss. Power amplifier will need at least 1 mW power to work properly. Pre-amplifier is constructed from double clad Yb doped fibre is used to reduce the number of laser diodes spent on laser and nonlinear effects inside the fibre.

Pulses are stretched with 90 m stretch fibre to reduce nonlinearity during and after amplification. Stretching also increased the spectral width to 18 nm, as seen

from a diagnostics coupler (Figure 2.4).

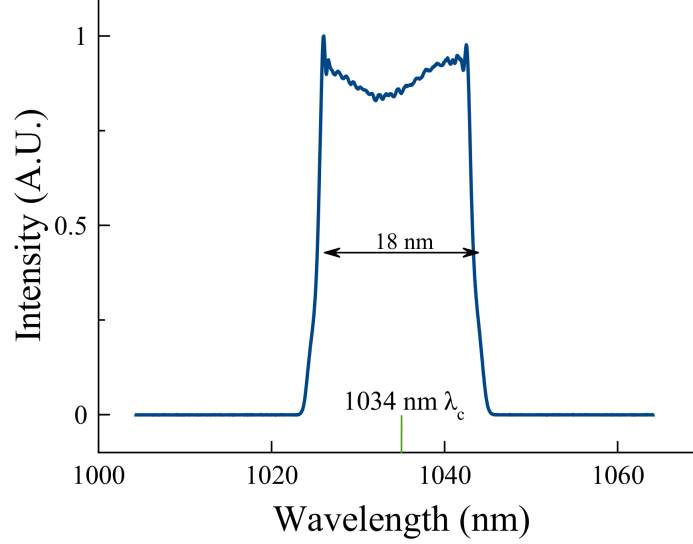


Figure 2.4: Coupler Spectrum after stretch fibre

Pre-amplifier was first constructed from single clad 6/125 Yb doped fibre. To reach the desired output power, fibre length had to be at least 5 meters. However, this lead to strong Raman stimulation which cause a huge wavelength shift and compression problems. So it had to be changed to double clad 20/125 fibre since pre-amplifier is wanted to be single stage. In the end, 1.5 meters of 20/125 Yb doped fibre for pre-amplifier is spliced. This provided 1.2 W output power. Spectral width increased to 25 nm.

Pre-amplifier pump diode current is supplied by 7.5V 13.6A power supply. PLD of pre-amplifier shares a 5V power supply with power amplifier PLD.

2.1.3 Power Amplifier

1.5 meters of Yb1200 20/125 is used as gain medium to increase absorption as keeping the nonlinearity manageable. After the free-space isolator, 2W output power at 400 kHz repetition rate is achieved.

Power amplifier current is also supplied by a separate 7.5V 13.6A supply. PLD

of power amplifier shares a 5V power supply with pre-amplifier PLD.

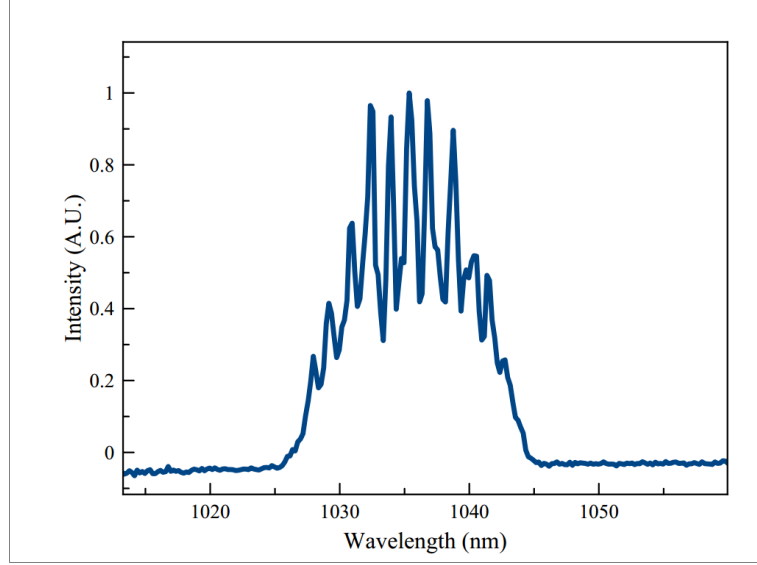


Figure 2.5: Laser Output Spectrum, 11 nm FWHM, 2 W output power, 63 ps

2.1.4 Compression and Laser Output

Compression is done by building a grating compressor with two gratings and a mirror (Fig. 2.6). Between two gratings pulses experience negative dispersion. Changing the distance between them determines the amount of negative dispersion they experienced. Details of grating compressor can be found from [43].

Gratings that are used have 900 lines/mm. Maximum efficiency for 900 lines/mm grating at 1035 nm centre wavelength is 28° incident angle to normal axis. Even slight changes at incident angle of light at any of the gratings will result in lower power efficiency. Thus it is very important to align gratings and mirrors associated with grating carefully. From dispersion calculations, the spacing between gratings found to be 70 cm, however precise adjustment was done by hand for the best compression. Maximum efficiency this compressor can reach is 65 % and 60 % is achieved in this system.

As energy of a pulse changes, they experience various amounts of nonlinearity so the grating optimization changes for each energy levels. However, after

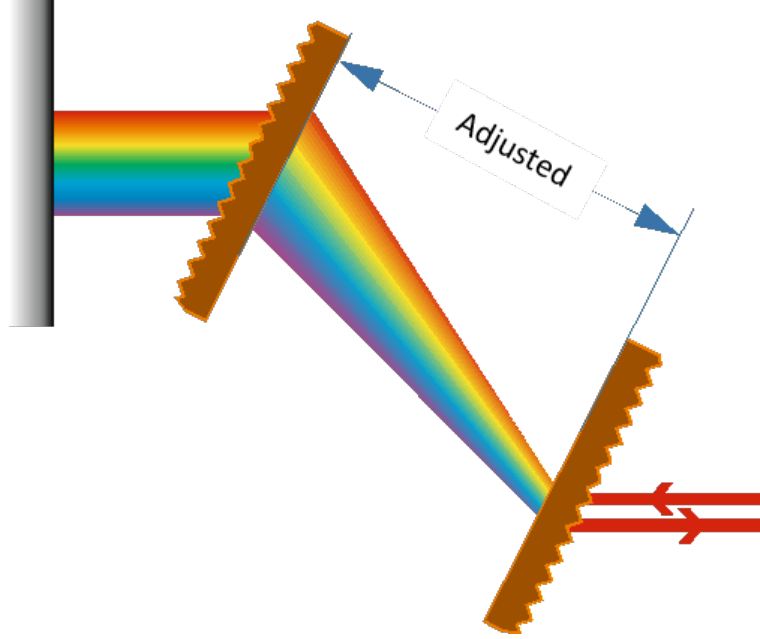


Figure 2.6: Incoming laser hits the first grating and its spectral components are separated spatially. With the help of second grating and mirror, each spectral component experience delay linearly proportional to their wavelengths, thus compressing the pulse temporally

optimizing for the highest pulse energy, change of compressed pulse width was negligible. At the output of compressor highest pulse width that measured is 300 fs FWHM for the desired range of pulse energies.

2.2 Electronics

Commercial diode drivers are used for both amplifiers and oscillator. Argon diode driver is used for oscillator diode. It is compact enough to fit under fibre platform and can supply up to 1 A which is more than enough for oscillator. It also has built in temperature controller for stabilization. Two PLDs are used for pre-amplifier and power amplifier. Those do not have active temperature stabilization but can supply much higher currents, up to 10 A.

Pulse picking between amplifiers is done with AOM driven by FPGA. BASYS2

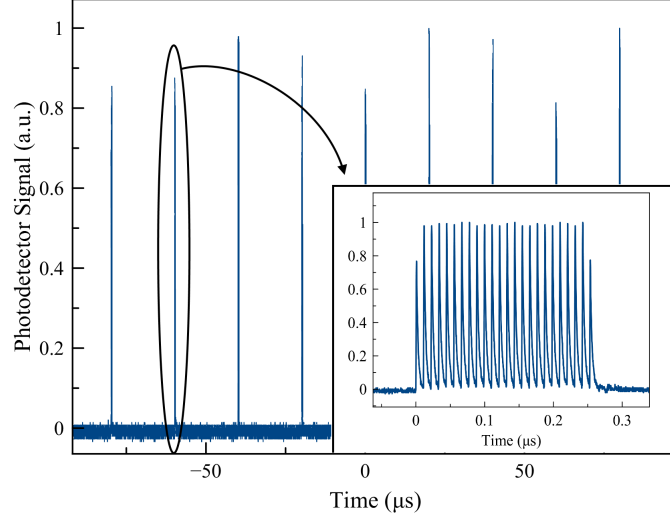


Figure 2.7: Burst Mode Operation(change for new oscillator)

is chosen for its low cost, no heavy computations are necessary for this application. A sensitive detector is connected to coupler output of the oscillator. Detector signal is between 0 V and 200 mV. However FPGA trigger is centred around 1 V. To overcome this, a DC BIAS circuit is built instead of an amplifier. It consists of a 1.25 V regulator and a DC BIAS from Mini Circuits (Fig. 2.8). With the help of a potentiometer, BIAS on detector signal can be adjusted to accordingly.

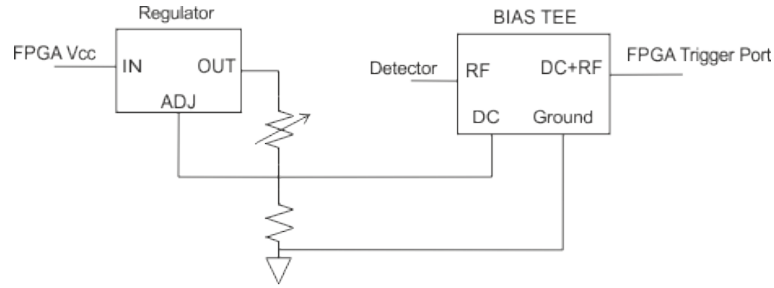


Figure 2.8: Potentiometer can adjust the DC bias from 0V to 2.7V. BASYS2 has its clocking threshold around 1.25V.

The detector output is connected to JC ports of the FPGA which have designated clocking routes for minimum skew. A VHDL program sends gates with desired width and frequency to AOM driver in order to pick any number of pulses at any repetition rate. Additionally, switches are programmed such that AOM modulation can set to full pass for diagnostics, burst-mode for applications and

uniform-mode for comparison with burst-mode. FPGA needs a separate 5 V, 5 A power supply to isolate it from high currents.

After boxing of the system there will be total of two 7.5V, 13A power supplies and three 5V, 5A power supplies.

2.3 Optical Coherence Tomography

Optical Coherence Tomography (OCT) is the most common imaging device for ophthalmologic applications since it presents non-invasive high resolution (equivalent to low-power microscope) 3D imaging in soft tissue.

OCT imaging is very similar to ultrasound which relies on broadband sound waves sent to tissue where different frequencies bounce off from corresponding depths (Fig. 2.9). Because it is based on light, the resolution is much higher than ultrasound. Detection is based on low coherence interferometry which greatly increases signal-to-noise ratio (SNR), creating clear images without background noise.

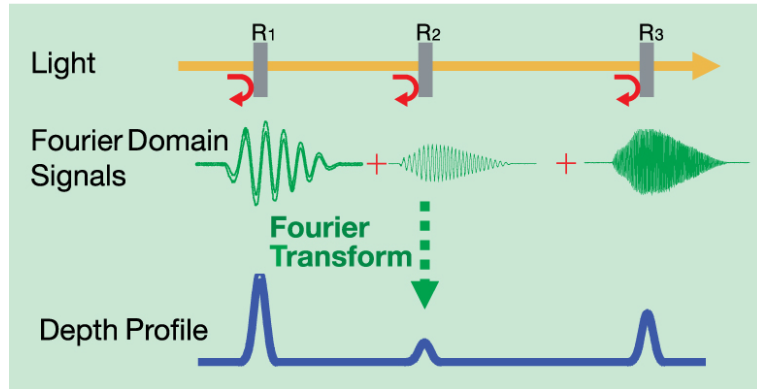


Figure 2.9: Different wavelengths reflected from corresponding depths and interfere with reference beam to construct the final image. Interference beam is measured by a detector array

The OCT in this system is a spectral domain OCT (SD-OCT). The interference pattern is detected by an array of detectors. The main disadvantage of

SD-OCT is its decreased signal-to-noise ratio as imaging point moves away from zero delay. Different depths reflect corresponding wavelengths if refractive index changes which interfere with reference light. Measure the interference pattern with an array of detectors provide necessary information to construct 1D depth image. Galvo scanner walk the beam to build up 2D or 3D images from many 1D images. CALLISTO OCT [44] is purchased from Thorlabs as OCT for integration to the system. Its central wavelength is at 930 nm (Super Luminescent diode). Maximum depth possible for imaging is 1.6 mm. It has $4\text{ }\mu\text{m}$ lateral resolution. It came with ThorImage OCT software to handle rendering and other operations regarding the imaging (Fig. 2.10). Moreover, the software development kit for OCT engine and OCT probe is ordered to be used in custom software development.

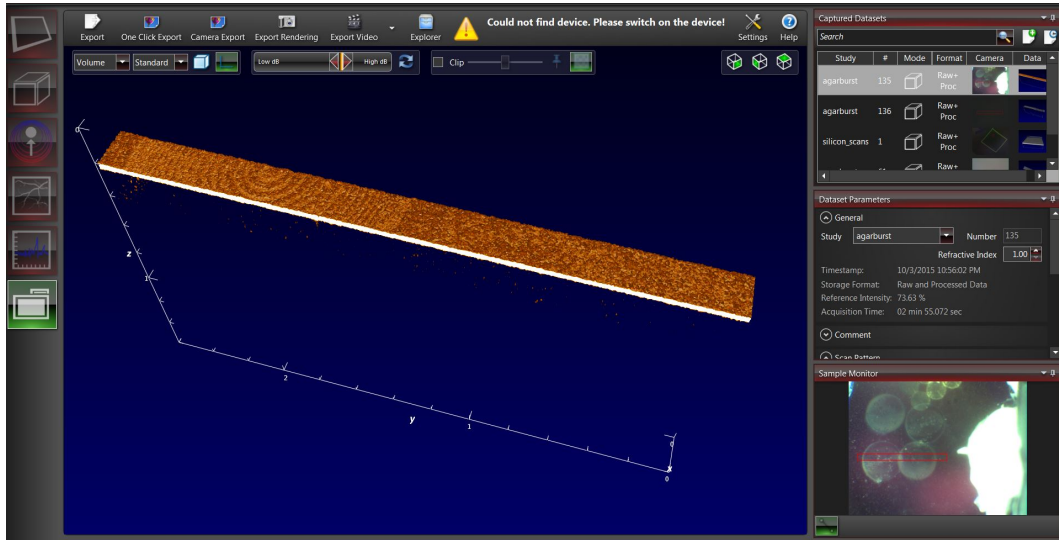


Figure 2.10: Screenshot of ThorImage OCT software. It handles the data coming from OCT engine. Imaging type, resolution, speed can be chosen. Real time camera feed can also be seen within ThorImage. It has some additional filters and processing to reduce the distortions.

Modular OCT probe is obtained for its freedom of modification. This is especially important since the processing laser beam should follow the same path with imaging beam which is only possible by modifying the probe.

The focal point of laser is found by using thin lame and moving OCT probe vertically at high power. When plasma on surface is visible, OCT reference arm

can be adjusted to any desired length. It is usually kept at 0 mm to be able to image the sample as deep as possible while processing.

2.3.1 Integration with Laser

Integration of the laser and OCT is essential to accurately target laser on the eye . Planar targeting is done by galvo scanner inside the OCT probe while vertical targeting is done by computerized elevator.

First of all, some modifications on modular probe is done for input laser beam. An additional cage containing a dichroic mirror is placed between galvo scanner and beam splitter. Angle of dichroic mirror is at 45 degrees to achieve maximum power efficiency from laser. With the help of 3 mirrors laser beam is carried along the bridge with elevator. Beam is coming to the top of OCT probe to prevent any interruptions from XY stage. Last mirror that directs the beam downwards should be aligned very carefully perpendicular to ground. Otherwise power may change with elevator movements (Fig. 2.11). After alignments, efficiency from laser output through compressor to target is measured to be 40%.

As a result, both imaging and processing beam follows the same path after additional dichroic mirror, thus allowing imaging and processing to be done one after the other without making any changes. This ensures more precise targeting with OCT images.

LSM03-BB lens is changed with LSM02-BB for sharper focus however it reduced our field of view (FOV). Due to galvo mirror sizes and f-theta lens on the probe, FOV is about 0.6 mm X 0.6 mm. Although it would not be sufficient for human eye surgery, it is enough for animal experiments.

The efficiency of the integration from compressor output to sample is 40%. It can deliver up to 4 μ J pulse energy on sample. Since the plan is to lower the pulse energy to sub μ J for processing, current efficiency should be enough.

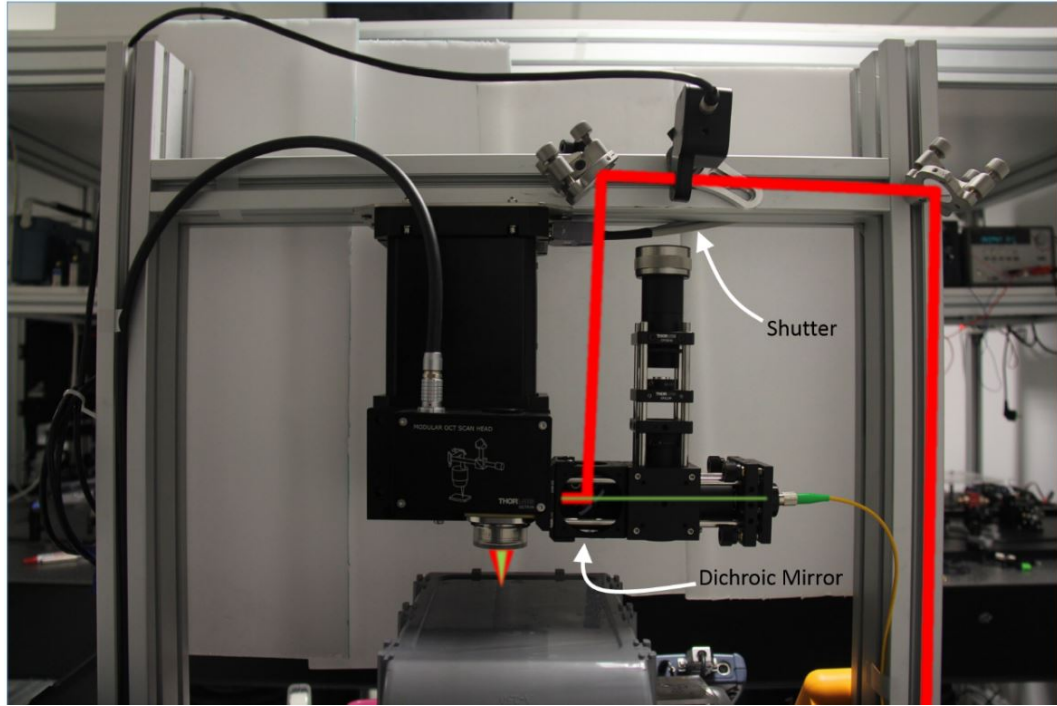


Figure 2.11: Processing beam (red) is inserted via dichroic mirror. Imaging beam (green) travels on its usual but elongated path. A programmable shutter is placed on path of processing beam.

2.4 Software

The system will be used by medical doctors who, are assumed to have no technical knowledge or background on operating a laser, galvo scanner or programming. A reliable and capable program with graphical user interface was necessary. A typical operation would require corneal incision, capsulotomy and lens fragmentation. So horizontal and vertical planes are to be created in straight or circular lines.

Thorlabs provided SpectralRadar.dll file for OCT which also can control the galvo scanner inside OCT probe independently. Thus, to avoid any compatibility issues that may rise, the software is written in C++. Integration of shutter and joystick depends on ActiveX. This way a user friendly GUI is also possible with ActiveX controls (Fig. 2.12).

The library works with arbitrary units of length which should be converted to real units. Some trial runs revealed that 1 unit of length of galvo corresponds to 0.5 mm with the lens and galvo integrated.

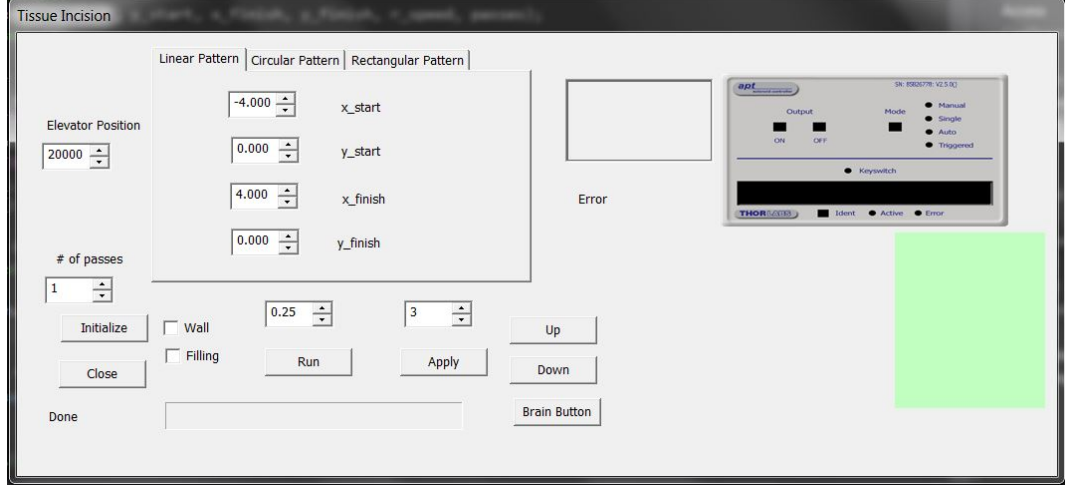


Figure 2.12: Screenshot of the software. One can choose between 3 predetermined patterns with 2 different options (wall structure & raster). It can also adjust the initial height of the elevator and the intensity of OCT probe lighting.

Every iteration of procedure starts with moving the elevator to desired height. Then the shutter opens for processing beam. Galvo scans the target with chosen pattern and its parameters. After that, shutter closes. It can be repeated with any number of times while changing some parameters in between iterations, i.e. elevator position to create complex patterns.

This software can operate galvo scanner in lines, raster pattern and concentric circles while changing the elevator position simultaneously for 3 dimensional targeting of focal point. Speed of galvo scanner can be adjusted via GUI. User can specify how many times to repeat chosen pattern. In the future, this software will be able to render OCT images and CCD camera feed on GUI without the need of commercial software of OCT that Thorlabs provided.

Chapter 3

Methodology

Adequacy of the laser was tested by a series of experiments. Both biological and non-biological were subject to experiments to compare the strengths and weaknesses of burst-mode with uniform-mode for this particular laser. Explanations of how these experiments were conducted are covered in this chapter.

3.1 Preparations

The focal point of laser is found by using thin lame and moving OCT probe vertically at high power. When plasma on surface is visible, OCT reference arm is adjusted to get the focus to any desired depth on OCT image. It is usually kept at 0 mm to be able to image the sample as deep as possible while processing. Experiments are done on either agar or bovine eyes.

In comparison experiments for uniform-mode with burst-mode, scanning speed is adjusted to create 50 % overlapping between bursts. For direct comparison to the uniform-mode, pulse energy is kept equal to the burst case and scanning speed is adjusted to keep the fluency same with burst-mode. So for 24-pulse bursts repeated at 50 kHz, the scanning speed is set to 0.2 m/s. 50 kHz burst

repetition rate is the lowest it can be set without experiencing Amplified Spontaneous Emission (ASE) generation. For same scanning speed, uniform-mode repetition rate is set to 1200 kHz at same individual pulse energy. To find the threshold pulse energy in each case of burst-mode and uniform-mode, the pulse energy was increased until continuous cutting occurred for each case.

3.2 Blood Agar Experiments

Agar gel is chosen for its similar optical and mechanical properties to soft tissue [45]. It is widely used as soft tissue phantom. Agar is prepared at 2 % density, 100 grams of water for 2 grams of agar. Solution is cooked with microwave for 2-3 minutes, while stirring ever 20 seconds for homogeneity. Then it is poured in to ice cube trays and refrigerated for 4 hours. After gels are solidified enough, they are kept in tap water inside refrigerator until they are needed. Once prepared, agar gels can be kept up to 2 weeks before the surface deteriorates.

Laser is tested with blood agar before moving on bovine eyes. Agar is placed in a culture dish filled with water to prevent drying out (Fig. 3.1). Drops of water is dripped on top occasionally. However, before processing, top surface is cleaned very softly with a lens cleaning tissue to reduce targeting errors since OCT cannot distinguish water from agar properly. One block of agar could stay under for 2 hours without changing before it starting to lose its physical properties.

These experiment is also done with various pulse energies to find an optimal point. The required pulse energy for agar experiments is higher than cornea so number of pulses is chosen to be per burst to be 8 at 50 kHz to increase individual pulse energy. Uniform mode repetition rate is adjusted to be 400 kHz respectively.

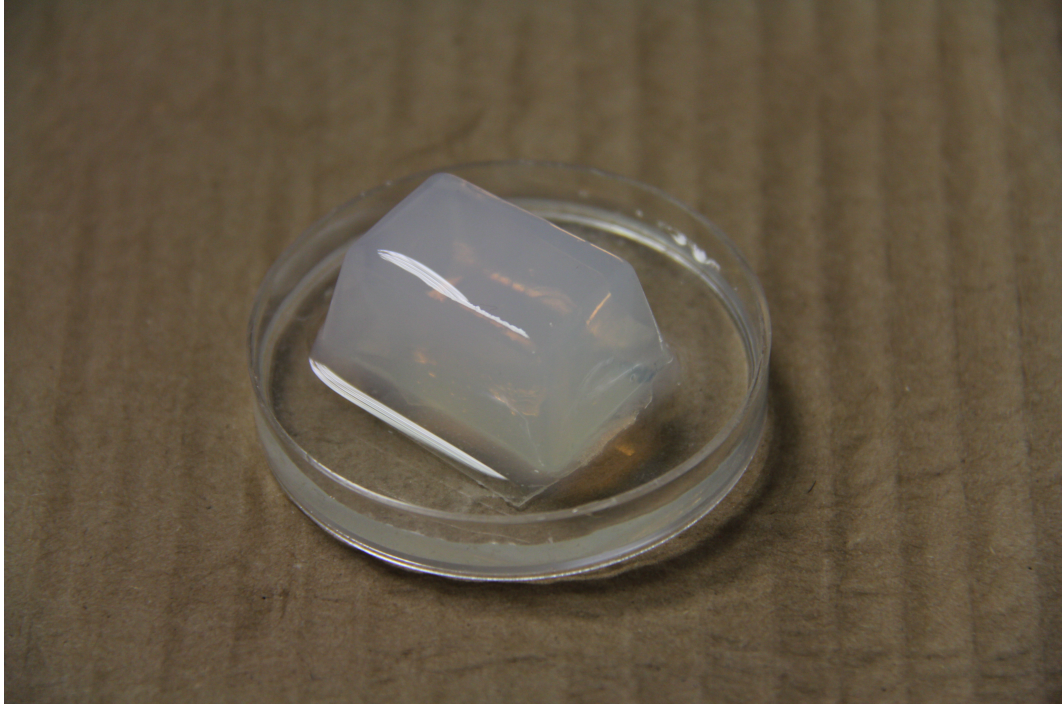


Figure 3.1: Agar is placed on petri dish filled with tap water. Occasionally, few drops of water is dripped on top to prevent drying out locally.

3.2.1 Straight Cuts

Creating ablation lines on surface with both uniform-mode and burst-mode was the first task to be done on agar. Scanning speed is set to 25 mm/s to get 50 % overlapping between bursts. Speed is not changed for uniform-mode to make a fair comparison. Various pulse energies are tested to find a pulse energy that can create smooth lines. A side by side comparison is made by OCT.

3.2.2 Volume Ablation

The system is tested if it is capable to perform patterns that are implemented in surgery properly. The aim was to remove a slice of agar from bulk, as done in refractive eye surgery [46]. It consists of two predetermined patterns, raster scan and spiral. Raster scan is applied on surface and imaged with OCT. Images show how much volume is ablated for a single pass with various pulse energy and scan

speeds.

3.3 PMMA Experiments

PMMA is determined to be the subject for observation of the effects of burst-mode and compare with uniform-mode, when processing occur below surface. The material is mostly transparent to infrared light so we can observe multi-photon absorption and test how threshold changes with burst-mode.

The distance between lines of raster scan is chosen to be 10 μm . Number of pulses for each burst is chosen to be 8, which is enough to observe the effects of burst mode barely. More pulses per burst would have been even better but that would push the laser to its limits. It may not be a concern in burst-mode but in uniform-mode, we couldn't go that high powers.

1 mm below surface of PMMA is chosen as focal point. Then 1mm x 1mm area is scanned with raster pattern. Scanning speed is set to 10 mm/s for both uniform-mode and burst-mode.

3.4 Bovine Eye Experiments (Corneal Flap)

Bovine cornea is used to test real world application of the cataract surgery system, if the parameters are fitting for such applications. Bovine eyes are collected directly from slaughterhouse and kept at -20°C in freezer. Cornea is extracted while the eye is still frozen with lancet. Then, it is unfrozen by putting in normal saline in room temperature. After this, cornea is soaked in glycerine to get rid of excess water.

After unfreezing the cornea it is inserted on to a holder where it is tightened and normal saline is pumped from beneath cornea (Fig. 3.2). A thin lame is placed on top of cornea with saline in between them. Surface tension and pumping

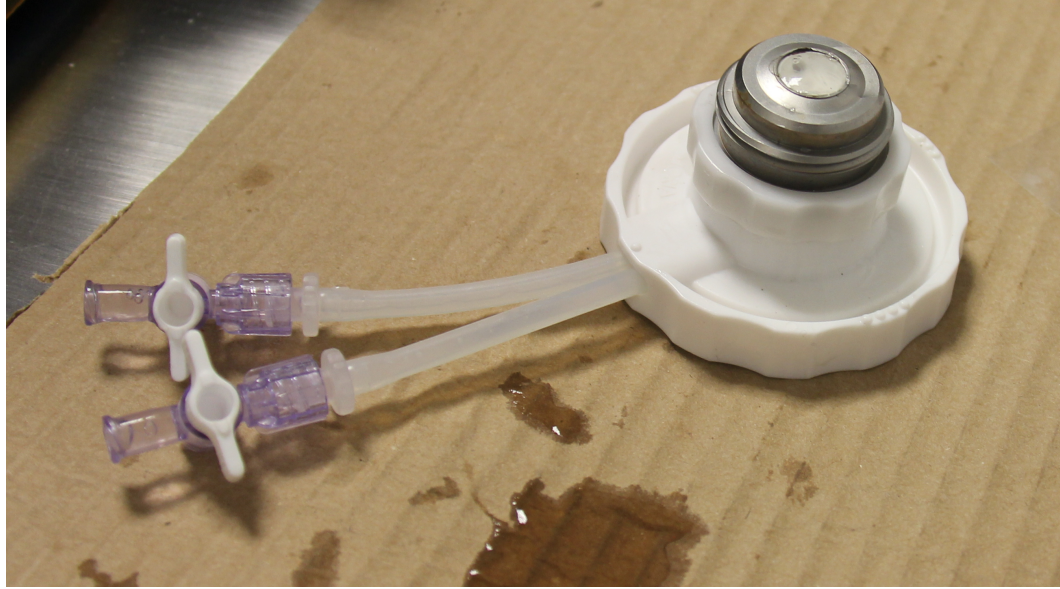


Figure 3.2: Extracted cornea is place on holder. Then it is tightened with a cap (gray). Normal saline is pumped from the tubes which prevents drying out.

keeps cornea in contact with normal saline all the time, preventing drying out. Holder is placed on an elevator for computer controlled z-axis movements. The experiments can be conducted for 1-2 hours before edema occurs in cornea and prevents the processing properly.

Formation of corneal flaps involved cutting concentric circles on horizontal plane first followed by a spring pattern in z direction in the cornea. Edge of biggest circle in former pattern intersect latter from bottom, so that they form shape of a coin. For the spring pattern, laser is focused beneath the bottom surface of cornea about 200 μm by using OCT imaging. Then, after scanning each straight line, cornea is lowered in steps of 5 μm cutting a line at each height until the top surface is reached (Fig. 3.3 (a)). This is repeated until the surface is reached. Then, concentric circles are applied on horizontal plane by aiming 200 μm beneath the top surface of cornea and scanning the laser where radius is reduced 10 μm each time so that consequent circles are touching each other (Fig. 3.3 (b)). Hence after the flap is created so, it is hold and lifted with toothed forceps and cut with stitch scissors. Imaging of the results are done with either reflective microscope or OCT.

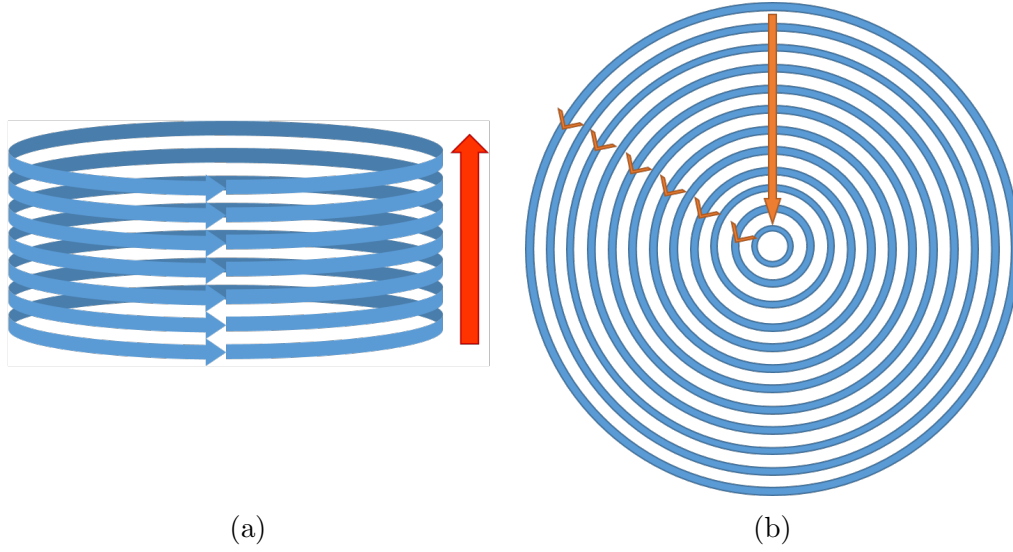


Figure 3.3: (a) A spring pattern starting from $200\ \mu$ below surface, as walls of the flap. (b) constructs the basis of the cap of corneal flap beneath the surface

After the processing, flap is detached with help of forceps, tweezers and spatula. If it is successfully detached, the flap is imaged first and then covered on eye again and place it inside formaldehyde to fixate it. Then the fixated samples are sent to laboratory in Kırıkkale University for histological analysis. Both the sides and base of the flap had no visible irregularities but histological report is still needed to have a better understanding of the damage.

Chapter 4

Results

4.1 Agar Experiments

Both uniform-mode and burst-mode managed to create smooth lines on agar. However, on a fair comparison, uniform-mode repetition rate had to be increased which in turn decreased pulse energy. 50 kHz repetition rate with 8 pulse per burst is taken equivalent to 400 kHz uniform-mode. In this case, the threshold was at $1.75 \mu\text{J}$ pulse energy for burst mode while uniform-mode failed to do any modifications on surface. Scanning speed is set to 2 m/s to get to see the effect of each burst or pulse.

As for volume ablation, scanning speed is reduced to get 50% overlapping between bursts. That corresponds to 0.25 m/s scan speed for 50 kHz burst repetition rate. Results were consistent with before. $1.5 \mu\text{J}$ is enough for burst-mode, which have 8 pulses per burst, while uniform-mode fails to do any visible modifications. At $1.75 \mu\text{J}$, burst-mode managed to ablate surface smoothly, yet, uniform-mode ablation lines were highly irregular (Fig. 4.2). Only after $3 \mu\text{J}$, uniform-mode could show its effect on agar, even though the lines are still irregular. These results are also consistent with findings of previously done experiments with burst-mode in agar [47].

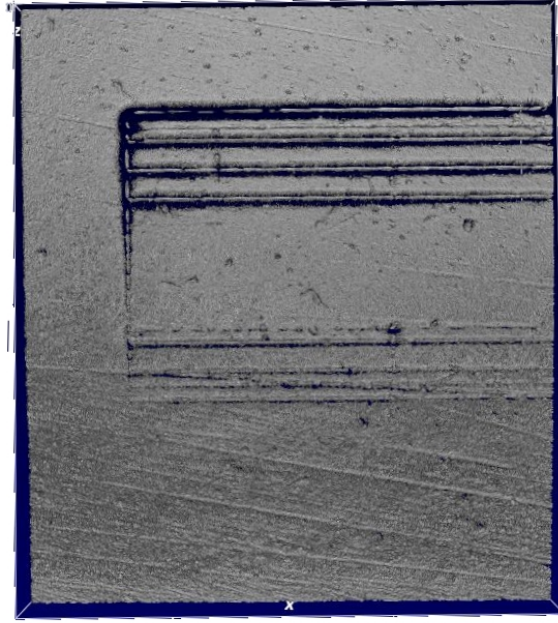


Figure 4.1: Lower half of agar is scanned with uniform-mode and upper half is scanned with burst-mode. There are little visible modification on uniform-mode side compared to burst-mode side, seen from OCT image while there are clearly ablation lines on burst-mode side. Pulse energy is kept at $1.7 \mu\text{J}$ in both cases.

4.2 PMMA Experiments

Uniform mode experiments failed to create proper ablated surface, or any ablation lines for that matter. The pulse energy was either too low to create any modification or average power is too high that it melts the material (Figure 4.3).

On the other hand, burst-mode have managed to create an ablated surface, with visible ablation lines at $2.5 \mu\text{J}$ pulse energy (Figure 4.4). There are some collateral damage as well but this is expected from PMMA which has scant elasticity.

It can be argued that burst-mode with this laser is capable of multi-photon processing where uniform-mode fails to do so. Uniform mode could either melt or

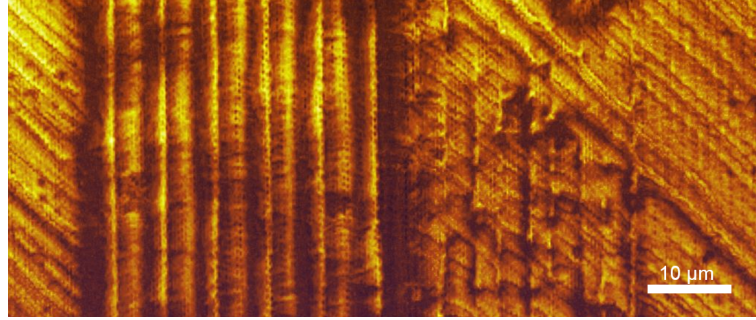


Figure 4.2: Half of agar is scanned with burst-mode (left side), $1.75 \mu\text{J}$ pulse energy and $10 \mu\text{m}$ separation between each line. Right side is scanned with exactly same parameters, except uniform-mode instead of burst-mode with 400 kHz repetition rate.

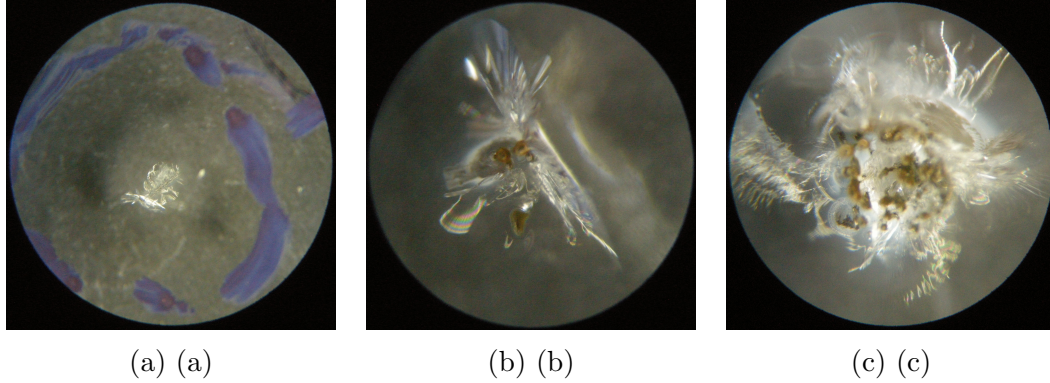


Figure 4.3: Uniform repetition rate at 400 kHz with pulse energies 900 mW, 1 W and 1.2 W respectively. Each of them is scanned with 10 mm/s

do no processing at all but burst-mode can create clean lines with little collateral damage.

4.3 Bovine Eye Experiments (Corneal Flap)

Virtually no difference in quality of the cuts detected as laser focus go towards to surface in spiral pattern. So pulse energy is kept same during entire procedure. As expected, similar pulse energies that was found effective for agar also worked on cornea. In fact, ablation threshold for cornea was lower than agar. Subsurface modifications on agar were already done so it is known those pulse energies will

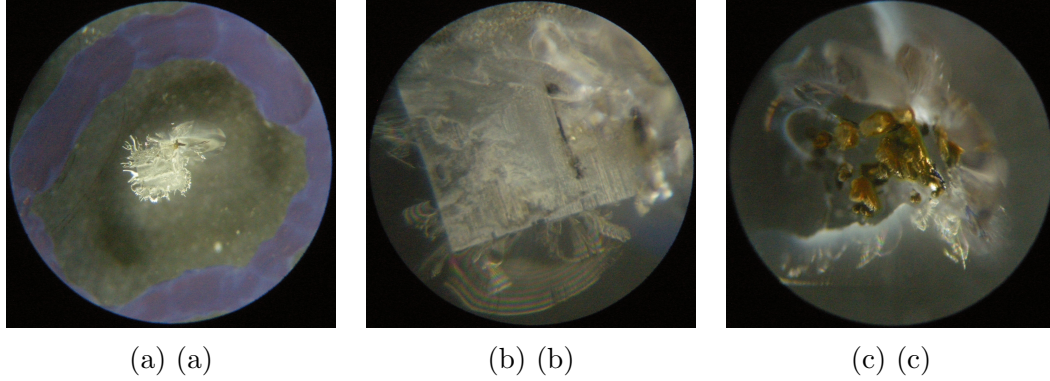


Figure 4.4: 8 pulse per burst with pulse energies 900mW, 1W and 1.2W. Each of them scanned with 10 mm/s with 50 kHz burst repetition rate

be enough.

In order to utilize the advantages of burst-mode, the number of pulses per burst were increased to 16, 24 and 48. Both 16 and 24 pulse per burst managed to create corneal flaps but, 48 pulse per burst failed to do so. Pulse energies are decreased proportionally with number of pulses. As a result, individual pulse energy for 48 pulse per burst case became so low that critical energy for ablation is never exceeded.

The corneal flaps are created with 24 pulse (Fig. 4.5) per burst since this reduced the pulse energy most. Threshold for 24 pulse per burst found to be $0.8 \mu\text{J}$ for $10 \mu\text{m}$ spot diameter. Uniform-mode operation failed to do any visible processing with even $1 \mu\text{J}$ pulse energy. In literature, the photodisruption threshold was reported to be $2\text{-}4 \mu\text{J}$ with $5 \mu\text{m}$ spot diameter and 200 fs pulse width [19]. Pulse intensity at focus is reduced by a factor of ~ 15 with burst-mode operation compared to that result with uniform-mode operation.

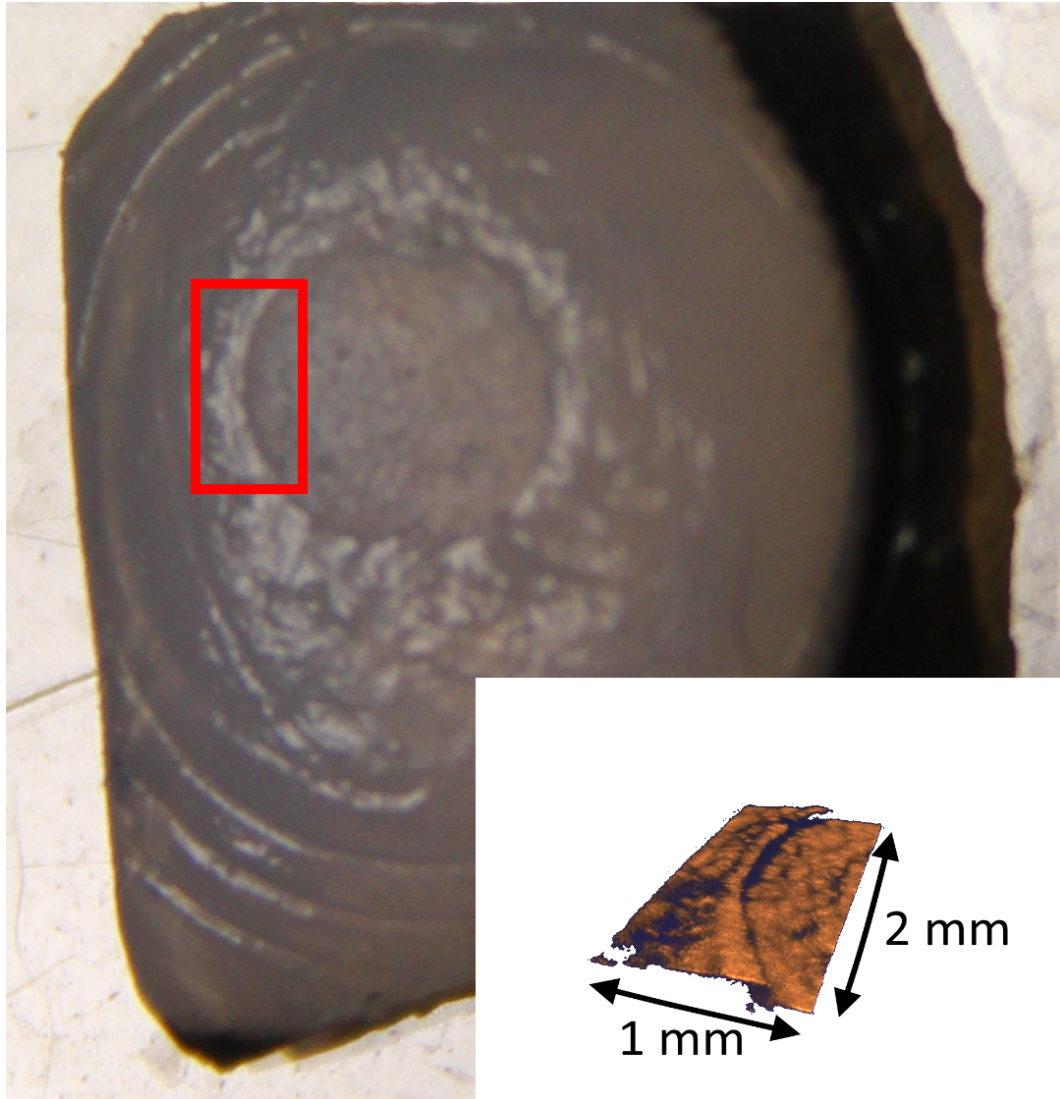


Figure 4.5: 24 pulse per burst, 833 nJ pulse energy, repeated at 50 kHz.

Chapter 5

Conclusion

With this thesis, refractive laser-assisted cataract surgery is provided a new tool, namely, a femtosecond laser system that exploits the recently discovered ablation-cooling laser-material removal technique. To this end, a custom Yb fibre laser was built with MOPA architecture that can produce up to 10 μJ pulse energies with 12 nm spectral width and less than 300 fs FWHM after compression. The oscillator repetition rate is 91 MHz. Burst-mode operation is enabled with AOM which is modulated by an FPGA. A detector is connected to diagnostics port of the oscillator to trigger FPGA in synchronize with the seed pulses. In order to extract as high energy as possible from the system in the material processing experiments, a burst repetition rate of 50 kHz was used, but not any lower due to concern for ASE generation. Uniform pulsed mode was also used to form a basis of comparison of processing quality and efficiency with burst mode. The uniform mode parameters were set to obtain equivalent effective repetition rate and fluency incident on sample.

The OCT system is integrated to the laser system for non-invasive imaging prior to and after processing. It has broadband super luminescence diode centered at 930 nm as a source and can measure 1.6 mm depth, with 8 μm lateral and axial resolution. Probe of OCT consists of a reference arm, camera, f-theta lens, galvo scanner and beam splitter. Modular probe is purchased and modified to obtain

overlapping laser beam with imaging beam. F-theta lens of the galvo scanner is changed to get a sharper focus of 10 μm diameter on sample which increased lateral resolution to 4 μm while decreasing focal distance and FOV. New lens has reduced focal length from 3.6 cm to 1.8 cm. After the integration, 40% efficiency on sample from laser output is achieved. Switching between imaging and processing can be done seamlessly since they both follow same optical path and don't require any extra preparation steps to switch. Finally, a custom software is written in C++ to control galvo scanner inside OCT probe, elevator and shutter to run the experiments.

Using fibre laser instead of solid-state laser in surgery system can reduce the cost of laser assisted cataract surgery, making it potentially more easily affordable to hospitals and patients who were not able to afford surgery before. Reduced costs of fibre lasers compared to solid state lasers alone makes this system likely to be preferred over current laser assisted cataract surgery systems.

Preliminary experiments were done on either blood agar, PMMA or extracted bovine eyes. The purpose of blood agar experiments was to test laser system capability for photo disruption. PMMA experiments were to investigate the effectiveness of burst mode and its advantages over uniform mode. Finally, bovine eye experiments are conducted as proof of concept that this laser system is capable of performing ophthalmic surgeries with burst mode.

The experiment results demonstrated the overall superiority of the ablation cooled regime. While both modes managed to create ablation on cornea and agar, uniform-mode operation produced irregular, unsatisfactory cuts at 1.7 μJ and burst mode showed smooth ablation lines. Furthermore, pulse energy threshold for processing was improved. Uniform-mode operation threshold was 3 μJ , on the other hand, burst-mode operation reduced the threshold to 1.2 μJ . In addition to that, in PMMA, burst-mode managed to ablation lines under surface without significant carbonization. However, uniform-mode either burnt the area or did no processing at all. This suggests that burst-mode has changed the physics behind the nonlinear absorption process. Finally, when it comes to create a corneal flap, laser operated only on burst-mode as its superiority is already proved. The real

challenged has occurred in removing the flap with tweezers rather than creating the cuts with laser.

Fluency for photo disruption is improved by a factor of ~ 15 compared to threshold reported in literature [19]. It is expected to reduce the possibility of complications after surgery by reducing the heating.

This system can be used to conduct animal experiments and proof of concept research but is insufficient for human trials. Especially OCT imaging depth, speed and galvo field of view need to be increased. In addition to that a proper boxing design that exploits flexibility of fibres is required to have much smaller form factor, however, an integration into an experimental prototype will be realized for preclinical trials on animals to be conducted by doctors in the hospital environment.

Bibliography

- [1] C. Kerse, H. Kalaycioglu, P. Elahi, S. Yavas, D. K. Kesim, O. Akcaalan, B. Cetin, B. Oktem, M. D. Asik, H. Hoogland, R. Holzwarth, and F. O. Ilday, “Ablation-cooled material removal with ultrafast bursts of pulses,” *Submitted to Nature*, 2016.
- [2] P. A. Asbell, I. Dualan, J. Mindel, D. Brocks, M. Ahmad, and S. Epstein, “Age-related cataract,” *The Lancet*, vol. 365, no. 9459, pp. 599–609, 2005.
- [3] A. Spector and W. H. Garner, “Hydrogen peroxide and human cataract,” *Experimental Eye Research*, vol. 33, pp. 673–681, December 1981.
- [4] H. Cheng, “Causes of cataract.,” *BMJ*, vol. 298, no. 6686, pp. 1470–1471, 1989.
- [5] B. E. Klein, R. Klein, and K. E. Lee, “Incidence of age-related cataract: the beaver dam eye study,” *Archives of Ophthalmology*, vol. 116, no. 2, pp. 219–225, 1998.
- [6] O. Chestnov, “Universal eye health: a global action plan 2014-2019.” http://www.who.int/blindness/AP2014_19_English.pdf?ua=1, 2013. Accessed: 2015-12-21.
- [7] G. Munton, “A short history of cataract surgery,” *CE Optometry*, vol. 4, no. 2, pp. 45–88, 2001.
- [8] H. Ridley, “Intra-ocular acrylic lenses: a recent development in the surgery of cataract,” *The British Journal of Ophthalmology*, vol. 36, no. 3, p. 113, 1952.

- [9] C. Binkhorst, “The iridocapsular (two-loop) lens and the iris-clip (four-loop) lens in pseudophakia,” *Transactions - American Academy of Ophthalmology and Otolaryngology*, vol. 77, no. 589, p. 9, 1973.
- [10] C. D. Kelman, “Phaco-emulsification and aspiration : A new technique of cataract removal: A preliminary report,” *American Journal of Ophthalmology*, vol. 64, pp. 23–35, July 1967.
- [11] F. Fankhauser, E. van der Zypen, and P. Roussel, “Method for the surgical treatment of the eye,” July 5 1983. US Patent 4,391,275.
- [12] Z. Nagy, A. Takacs, T. Filkorn, and M. Sarayba, “Initial clinical evaluation of an intraocular femtosecond laser in cataract surgery,” *Journal of Refractive Surgery*, vol. 25, no. 12, p. 1053, 2009.
- [13] I. Alcon LenSx, *LenSx Laser System Operator’s Manual*, 2011.
- [14] L. Probst and C. Chan, *Femtosecond Cataract Surgery: A Primer*. Slack Books, 2012.
- [15] Optimedica, “Catalys laser femtosegundo para cirurgia de cataratas,” 2011.
- [16] K. E. Donaldson and et al., “Femtosecond laser assisted cataract surgery,” *J Caratact Refract Surg*, vol. 39, pp. 1753–1763, 2013.
- [17] M. H. Niemz, *Laser-tissue interactions: fundamentals and applications*. Springer Science & Business Media, 2013.
- [18] G. R. Osche, “Optical detection theory for laser applications,” *Optical Detection Theory for Laser Applications, by Gregory R. Osche, pp. 424. ISBN 0-471-22411-1. Wiley-VCH, July 2002.*, vol. 1, 2002.
- [19] T. Juhasz, F. H. Loesel, R. M. Kurtz, C. Horvath, J. F. Bille, and G. Mourou, “Corneal refractive surgery with femtosecond lasers,” *Selected Topics in Quantum Electronics, IEEE Journal of*, vol. 5, no. 4, pp. 902–910, 1999.
- [20] P. J. Keller, A. D. Schmidt, J. Wittbrodt, and E. H. Stelzer, “Reconstruction of zebrafish early embryonic development by scanned light sheet microscopy,” *Science*, vol. 322, no. 5904, pp. 1065–1069, 2008.

- [21] M. Deubel, G. Von Freymann, M. Wegener, S. Pereira, K. Busch, and C. M. Soukoulis, “Direct laser writing of three-dimensional photonic-crystal templates for telecommunications,” *Nature Materials*, vol. 3, no. 7, pp. 444–447, 2004.
- [22] J. R. Cook and J. R. Albertine, “The navy’s high-energy laser weapon system,” in *Photonics West’97*, pp. 264–271, International Society for Optics and Photonics, 1997.
- [23] J. P. Dowling, M. Scalora, M. J. Bloemer, and C. M. Bowden, “The photonic band edge laser: A new approach to gain enhancement,” *Journal of Applied Physics*, vol. 75, no. 4, pp. 1896–1899, 1994.
- [24] T. H. Maiman, “Stimulated optical emission in ruby,” in *Journal of the Optical Society of America*, vol. 50, pp. 1134–1134, 1960.
- [25] S. Strauf, K. Hennessy, M. Rakher, Y.-S. Choi, A. Badolato, L. Andreani, E. Hu, P. Petroff, and D. Bouwmeester, “Self-tuned quantum dot gain in photonic crystal lasers,” *Physical Review Letters*, vol. 96, no. 12, p. 127404, 2006.
- [26] J. L. Jewell, J. Harbison, A. Scherer, Y. Lee, and L. Florez, “Vertical-cavity surface-emitting lasers: design, growth, fabrication, characterization,” *IEEE Journal of Quantum Electronics*, vol. 27, no. 6, pp. 1332–1346, 1991.
- [27] B. Oktem, C. Ülgüdür, and F. Ö. Ilday, “Soliton–similariton fibre laser,” *Nature Photonics*, vol. 4, no. 5, pp. 307–311, 2010.
- [28] P. Willmott and J. Huber, “Pulsed laser vaporization and deposition,” *Reviews of Modern Physics*, vol. 72, no. 1, p. 315, 2000.
- [29] E. Ippen, C. Shank, and A. Dienes, “Passive mode locking of the cw dye laser,” *Applied Physics Letters*, vol. 21, no. 8, pp. 348–350, 1972.
- [30] H. Haus *et al.*, “Theory of mode locking with a slow saturable absorber,” *Quantum Electronics, IEEE Journal of*, vol. 11, no. 9, pp. 736–746, 1975.
- [31] D. Strickland and M. Gerard, “Compression of amplified chirped optical pulses,” *Optics Communications*, vol. 56, no. 3, pp. 219–221, 1985.

- [32] H. Lubatschowski, R. R. Krueger, and D. Smadja, *Textbook of Refractive Laser Assisted Cataract Surgery (ReLACS)*. Springer New York, 2013.
- [33] B. Stuart, M. Feit, S. Herman, A. Rubenchik, B. Shore, and M. Perry, “Nanosecond-to-femtosecond laser-induced breakdown in dielectrics,” *Physical Review B*, vol. 53, no. 4, p. 1749, 1996.
- [34] A. Ancona, F. Röser, K. Rademaker, J. Limpert, S. Nolte, and A. Tünnermann, “High speed laser drilling of metals using a high repetition rate, high average power ultrafast fiber cpa system,” *Optics Express*, vol. 16, no. 12, pp. 8958–8968, 2008.
- [35] C. Kerse, H. Kalaycioglu, F. O. Ilday, and E. Atalar, eds., *Nonthermal Material and Tissue Processing with 100 MHz*, 2012.
- [36] G. P. Sutton and O. Biblarz, *Rocket propulsion elements*. John Wiley & Sons, 2010.
- [37] W. M. Rohsenow, J. P. Hartnett, Y. I. Cho, *et al.*, *Handbook of heat transfer*, vol. 3. McGraw-Hill New York, 1998.
- [38] R. S. Marjoribanks, C. Dille, J. E. Schoenly, L. Mckinney, P. Kaifosh, P. Forrester, and Z. Qian, “Ablation and thermal effects in treatment of hard and soft materials and biotissues using ultrafast-laser pulse-train bursts,” *Photonics and Lasers in Medicine*, vol. 1, no. 3, pp. 155–169, 2012.
- [39] H. Kalaycioglu, K. Eken, and F. Ilday, “Fiber amplification of pulse bursts up to 20 μ J pulse energy at 1 kHz repetition rate,” *Optics Letters*, vol. 36, no. 17, pp. 3383–3385, 2011.
- [40] W. Hu, Y. C. Shin, and G. King, “Modeling of multi-burst mode picosecond laser ablation for improved material removal rate,” *Applied Physics A*, vol. 98, no. 2, pp. 407–415, 2010.
- [41] H. Kalaycioglu, Y. Eldeniz, Ö. Akcaalan, S. Yavaş, K. Gürel, M. Efe, and F. Ilday, “1 mJ pulse bursts from a Yb-doped fiber amplifier,” *Optics letters*, vol. 37, no. 13, pp. 2586–2588, 2012.

- [42] A. Chong, J. Buckley, W. Renninger, and F. Wise, “All-normal-dispersion femtosecond fiber laser,” *Optics Express*, vol. 14, no. 21, pp. 10095–10100, 2006.
- [43] E. Treacy, “Optical pulse compression with diffraction gratings,” *IEEE Journal of Quantum Electronics*, vol. QE-5, no. 9, pp. 454–458, 1969.
- [44] Thorlabs, *CALLISTO Spectral Domain OCT System Operating Manual*, 2011.
- [45] R. Cubeddu, A. Pifferi, P. Taroni, A. Torricelli, and G. Valentini, “A solid tissue phantom for photon migration studies,” *Physics in Medicine and Biology*, vol. 42, no. 10, p. 1971, 1997.
- [46] T. Sakimoto, M. I. Rosenblatt, and D. T. Azar, “Laser eye surgery for refractive errors,” *The Lancet*, vol. 367, no. 9520, pp. 1432–1447, 2006.
- [47] C. Kerse, H. Kalaycioglu, S. Yavas, O. Akcaalan, E. Atalar, and F. O. Ilday, “Non-thermal high speed tissue and material processing using a burst mode ultra-short pulsed fiber laser system.” GRC2014, 2014.

Appendix A

Detailed Laser Schematics

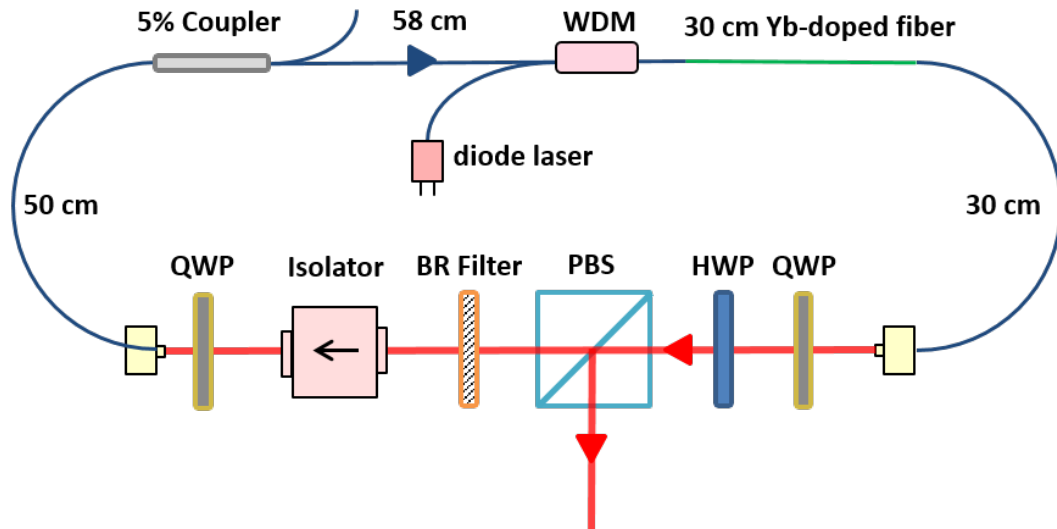


Figure A.1: Laser Oscillator

Diode of oscillator: 600mW temperature stabilized laser diode which operates at 976 nm single mode pump diode in oscillator.

Gain Fibre: Yb1200, 4 μm core, 125 μ cladding

WDM: Wavelength-division multiplexing, combines two different wavelengths into one fibre

Appendix B

XYZ Stage Details

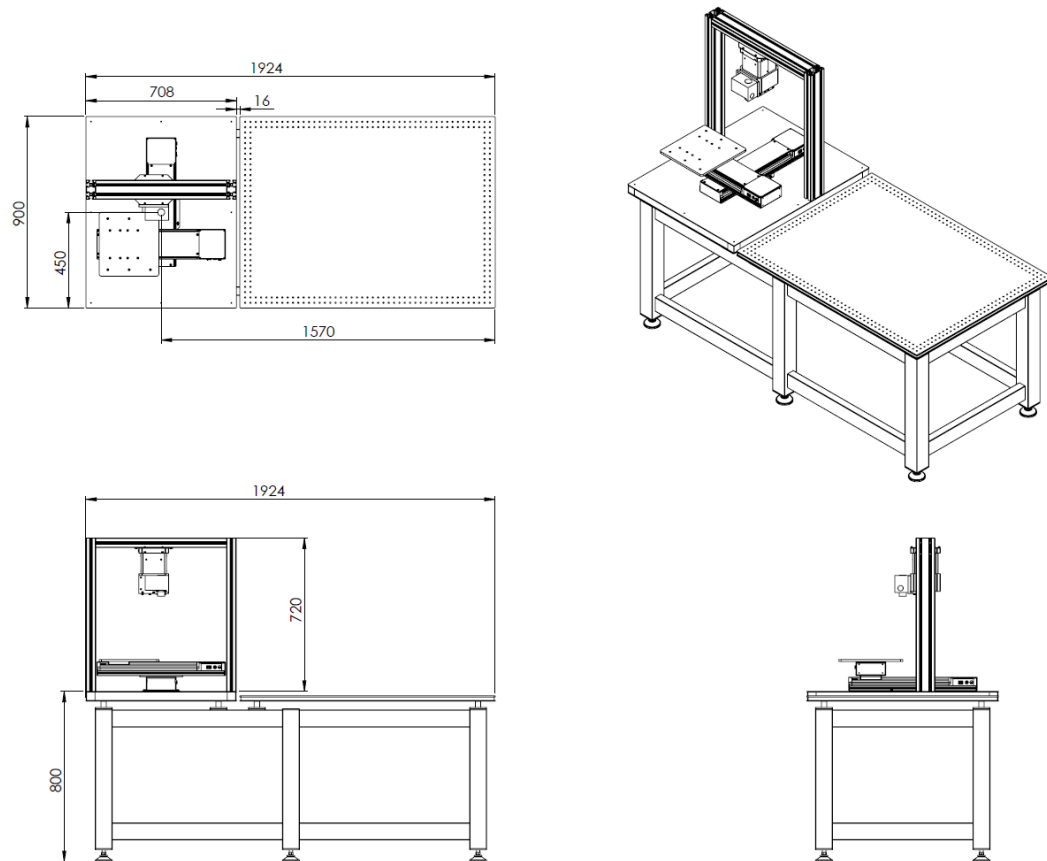


Figure B.1: Perspective drawings of XYZ stages, The table is able to fix both laser and XYZ stages and will be durable against perturbations.

B.1 Elevator (Z-stage)

Repeatability : 1 μm

Resolution : 0.1 μm

Precision : 4 μm

Maximum speed : 10 mm/s

Stroke : 7 cm

Controlled via RS232 serial port. Speed can be adjusted with "S" command. "DXXXXXXX" command sends the elevator to "XXXXXXX" position (X is decimal digit). It can be recalibrated with sending "H" command. Joystick function is enabled with "i" and "g" commands that moves elevator to up or down for 100 μm respectively.

B.2 XY Stage

A plate is fixed on it for samples to stand. X and Y axis of joystick corresponds to X stage and Y stage respectively. Stages start moving slow when a button is pressed. If button is held for 2 seconds, stage speeds up to allow fast positioning.